Coherent continuum generation above 100 eV driven by an ir parametric source in a two-color scheme

C. Vozzi,[1,*] F. Calegari,[1] F. Frassetto,[2] L. Poletto,[2] G. Sansone,[1] P. Villoresi,[2] M. Nisoli,[1] S. De Silvestri,[1] and S. Stagira[1]

[1]*National Laboratory for Ultrafast and Ultraintense Optical Science, CNR-INFM, and Department of Physics, Politecnico di Milano, Milan I-20133, Italy*

[2]*Laboratory for Ultraviolet and X-ray Optical Research, CNR-INFM, Università di Padova, Padova I-35131, Italy*

(Received 24 November 2008; published 26 March 2009)

High-order harmonics were generated in a two-color scheme exploiting an infrared parametric source with self-stabilization of the carrier-envelope phase. A significant cutoff extension was observed with respect to single color, 800 nm driving pulses at comparable peak intensities. Exploiting the wavelength tuning of the parametric source in the 1.5–1.6 μm range, a continuous xuv spectrum extending from 36 to 70 eV was generated in krypton. A broader xuv continuum, extending beyond 100 eV, was observed in argon. These results represent a step forward in the extension of attosecond science toward the soft x-rays region and open new perspectives in the investigation of quantum effects in atoms and molecules.

DOI: 10.1103/PhysRevA.79.033842 PACS number(s): 42.65.Ky, 42.65.Re, 42.65.Yj

I. INTRODUCTION

Since early experiments, high-order harmonic generation (HHG) has been suggested as a powerful table-top tool for temporal resolved measurements in the xuv spectral region with resolution ranging from the femtosecond to the attosecond domain. Big steps forward have been obtained in increasing the harmonic pulse intensity [1] as well as in extending the available harmonic spectral region [2]. Moreover, different techniques have been demonstrated for the generation of isolated attosecond pulses in the xuv exploiting HHG by carrier-envelope phase (CEP) stabilized laser sources [3,4].

The harmonic emission process can be easily understood in the framework of the three-step model [5]. The maximum achievable harmonic energy is given by $\hbar\omega_{\max}=I_P+3.2U_P$ [6], where I_P is the ionization potential of the gas target and $U_P \propto I\lambda^2$ is the quiver energy of the freed electron, with I and λ being the peak intensity and the wavelength of the driving field, respectively. Since $\omega_{\max}$ scales as λ^2, parametric sources operating in the ir have been proposed as a way to extend the harmonic emission spectrum up to keV energies [7–10]. The main drawback of this approach is the reduction of the harmonic yield expected with increasing driving wavelength [12–14].

Owing to the larger harmonic cutoff they provide, ir sources operating from 1.5 to 3 μm have been also suggested for the generation of isolated attosecond pulses exceeding 100 eV photon energy [15]. In order to generate such pulses in a reproducible way, it is necessary to confine the xuv emission within a single event, thus obtaining the generation of a continuous xuv spectrum. This temporal confinement can be achieved in several ways. One approach is the spectral selection of the cutoff region [16]. Another way exploits the strong dependence of harmonic generation on the polarization of the driving field [3,17]. A temporal gate of the harmonic emission can also be obtained in a *two-color scheme*, where the driving electric field is the superposition of two few-cycle pulses: one at frequency ω_0 and another at frequency $\omega_1=2\omega_0$ [18,19]. Recently Merdji *et al.* [20] theoretically demonstrated generation of isolated attosecond pulses in HHG driven by a multicycle two-color field with two components of comparable intensity: one at frequency ω_0 and the other one at a frequency ω_1 slightly detuned from the second harmonic. Kim *et al.* [21] proposed another approach, where isolated attosecond pulses are generated by a multicycle two-color field with a strong component at 800 nm and a weak one in the ir region. It is worth noting that CEP stability is a crucial prerequisite for driving pulses exploiting all these techniques. Triggered by this purpose, several high-energy infrared sources with passive CEP stabilization [22] have been developed for driving high-order harmonic generation processes [23–27].

In this work we report on the generation of a coherent continuous spectrum extending from 36 eV to more than 100 eV exploiting a self-phase-stabilized ir parametric source. This result was achieved in three steps: (i) xuv spectra were generated in atomic and molecular gases by the ir source. As expected, a significant cutoff extension was observed in all the targets with respect to 800 nm driving pulses; a preliminary estimation of the xuv emission intensity confirmed the yield scaling on driving wavelength reported in the literature. (ii) The wavelength tunability of the ir source was subsequently demonstrated in the 1.5–1.6 μm range, allowing full tunability of the harmonic peaks above 25 eV photon energy. (iii) Such tunability was then exploited for controlling the harmonic emission process in a two-color configuration, experimentally demonstrating the approach introduced in Ref. [20]. Such technique allowed us to generate *single-shot* broad xuv continua in krypton, extending from 36 to 70 eV. More interesting, though preliminary, results were obtained in argon, where a single-shot continuum extension beyond 100 eV was observed at the expense of a lower emission intensity. The combination of our experimental results opens new and encouraging perspectives for the extension of attosecond physics toward the soft x ray spectral region and for the investigation of quantum effects in atoms

*caterina.vozzi@polimi.it

and molecules in an unexplored photon energy range.

The paper is organized as follows. In Sec. II we briefly describe the experimental setup. In Sec. III we compare harmonic emission driven by the parametric ir source in atomic and molecular gases to that obtained by a standard Ti:sapphire laser. Results concerning HHG experiments in two-color configuration are reported in Sec. IV. Finally, we summarize the results in the conclusions.

II. EXPERIMENTAL SETUP

The ir parametric source exploited in our experiments is pumped by an amplified Ti:sapphire laser system (60 fs, 800 nm, 10 Hz, 120 mJ maximum pulse energy). In the present configuration a small portion of the available energy (~12 mJ) was used to drive the ir source. A broadband supercontinuum is generated by filamentation in a krypton-filled gas cell and a phase stable seed is then produced by difference frequency (DF) of the supercontinuum spectral components. This seed is then amplified through a two-stage optical parametric amplifier up to 1.2 mJ with a nearly transform-limited pulse duration of ~18 fs [27]. Carrier-envelope-phase stability of this source has been demonstrated, with rms fluctuations in the order of 220 mrad over 30 s [28]. The central wavelength of the amplified DF can be tuned between 1.4 and 1.6 μm without significantly affecting pulse duration and energy. In order to produce high-order harmonic radiation we focused the ir driving pulses on a synchronized gas jet operating at 10 Hz. Characterization of harmonic emission was performed by means of a soft x-ray spectrometer and a microchannel plate coupled to a phosphor screen and a charge coupled device (CCD) camera. In this configuration, the spectrometer is set to detect the spectral range between 36 and 150 eV. The harmonic structure is resolved only on a portion of the spectrum due to the finite instrumental resolution. Taking into account the spectrometer dispersion law and the properties of the detection system, we roughly estimated the maximum photon energy for which the harmonic structure could be resolved as ~115 eV for 800 nm driving pulses and ~79 eV for 1.5 μm driving pulses.

III. HHG IN SINGLE-COLOR SCHEME

As a preliminary step we investigated the capability of the ir parametric source in extending the harmonic emission above the 100 eV spectral region. Thus we compared the harmonic radiation generated by the 1.5 μm parametric source to harmonic spectra obtained with standard 800 nm driving pulses. For this purpose, a small portion of our Ti:sapphire laser system was used for generating harmonics with the same detection apparatus. The energy of the 800 nm pulses was reduced in order to get comparable pulse peak intensities in the focal region for both sources.

Figure 1 shows a comparison between normalized harmonic spectra (in logarithmic scale) generated in krypton (a) and argon (b) by the 800 nm laser and by the 1.5 μm source [(c) and (d), respectively]. The peak intensity of the 1.5 μm pulse at focus was estimated in about 2×10^{14} W/cm^2, whereas the focal peak intensity of the 800 nm pulse was

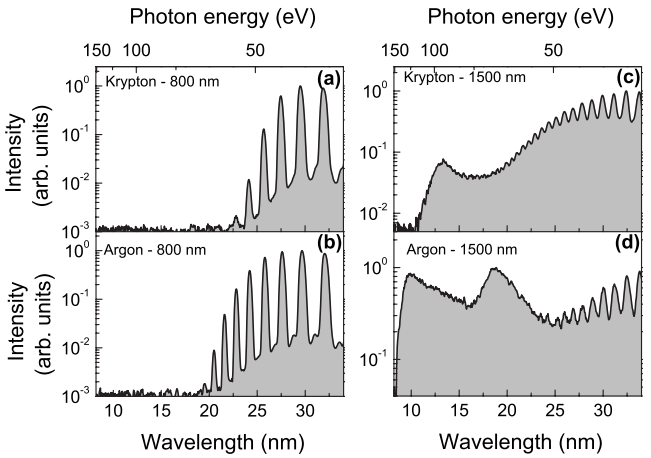

FIG. 1. Normalized high-order harmonic spectra generated by 800 nm driving pulses in (a) krypton and (b) argon. Normalized high-order harmonic spectra generated by 1.5 μm driving pulses in (c) krypton and (d) argon. All the spectra are in logarithmic scale.

about 2.6×10^{14} W/cm^2. A noticeable spectral extension of harmonic radiation was measured for the parametric source with respect to the standard Ti:sapphire source in both gases. Cutoff energy was 118 eV in krypton and 145 eV in argon for the 1.5 μm driving pulses; these values have to be compared to 54 eV for krypton and 64 eV for argon in the case of 800 nm driving pulses. The observed cutoff energies in argon agree with the prediction of the three-step model (65 eV for 800 nm driving pulse and 149 eV for 1.5 μm driving pulse at the considered peak intensities). It is worth noting that, in the present spectrometer configuration, the 1.5 μm driving pulse cutoff coincides with the detection instrumental limit; nevertheless, as one can see from Fig. 1, the spectral evolution suggests an extension beyond this value. In the case of krypton, we observed a difference between experimental cutoff energies and values predicted by the cutoff law (63 eV for 800 nm driving pulse and 147 eV for 1.5 μm driving pulse at the mentioned peak intensities). Such a difference could be ascribed to ionization saturation: the atomic medium is depleted before the peak of the driving electric field is reached, thus resulting in an effective peak intensity which is lower than the real one. Aside from the cutoff energy increase, harmonic spectra generated by the 1.5 μm driving source present interesting spectral feature. Indeed for both generating media the xuv spectra show deep modulations depending on the harmonic photon energy. These spectral structures seem not be related to absorption in the generating medium. Both single atom and collective effects are probably involved in determining these spectral features [11].

In order to investigate the behavior of the harmonic yield as a function of the driving wavelength, we compared harmonic emission in argon for the spectral region between 40 and 55 eV (where both driving pulses produce harmonics). We observed a decrease in the emission yield with increasing driving wavelength, which is comparable to the theoretical prediction in [12] and the experimental observation in [14]. In particular, our measurements show that the emission yield in the case of 1.5 μm driving pulses is about 2 orders of magnitude lower than the one observed with 800 nm driving

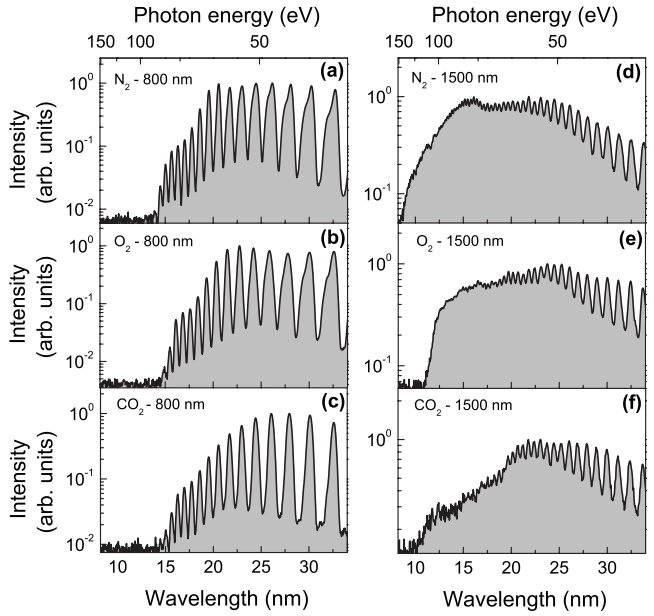

FIG. 2. Left panel: normalized high-order harmonic spectra generated by 800nm driving pulses in (a) N_2, (b) O_2, and (c) CO_2. Right panel: normalized high-order harmonic spectra generated by 1500 nm driving pulses in (d) N_2, (e) O_2, and (f) CO_2. All the spectra are in logarithmic scale.

pulses at comparable peak intensity. In order to take into account the experimental difference in the pulse peak intensity of the two driving beams we assumed that the nonlinear dipole moment matrix element d_{nl} depends on the driving pulse intensity I as $d_{nl} \propto I^5$ for plateau harmonics [29]. Then we found a scaling law for the harmonic yield as λ^{-6}. As a matter of fact, this result must be considered with some care, since a proper estimation of the yield scaling law with driving wavelength should take into account macroscopic effects. In our experiment we kept the argon gas pressure constant and we optimized the gas jet position in order to maximize the harmonic spectral extension; thus the phase matching influence on the estimation of harmonic yield is not easily discernible.

We extended our study to harmonic generation in molecular gases, namely, molecular nitrogen, molecular oxygen, and carbon dioxide. Left panel of Fig. 2 shows normalized harmonic spectra (in logarithmic scale) generated by the 800 nm laser source in N_2 (a), O_2 (b), and CO_2 (c). These results have to be compared to those reported in the right panel of Fig. 2, where harmonic spectra generated by 1.5 μm driving pulses in N_2 (d), O_2 (e), and CO_2 (f) are reported. In these measurements, the ir pulse peak intensity in the focus was about 2×10^{14} W/cm^2, whereas the focal peak intensity of the 800 nm pulse was estimated in about 3.7×10^{14} W/cm^2. For N_2, the cutoff photon energy moves from 86 eV in the case of the 800 nm driving pulse up to 141 eV for the ir driving pulse. It is worth noting that we observed a considerable extension in the cutoff frequency even if the intensity of the parametric driving pulse is only slightly more than half the intensity of the 800 nm driving pulse. For O_2, the cutoff photon energy for the 800 nm driving pulse corresponds to 83 eV and it increases up to 111 eV for the 1.5 μm driving pulse, where an abrupt cutoff is observed. Analogous result is observed for CO_2: the cutoff position moves from 83 up to 120 eV. In this latter case the cutoff appears less pronounced.

Incidentally, we note that these results underline the possibility of exploiting HHG as a tool for investigating molecular properties. Indeed up to now all the experiments on HHG from molecular targets have been performed with 800 nm Ti:sapphire laser sources (see for instance [30–35]). As our measurements demonstrate, HHG in molecular gases by near-ir driving pulses enters in a spectral region which was previously unexplored. This result is particularly important for relatively big molecules with a low ionization potential, since ionization saturation hinders high order harmonic generation in such molecules with standard Ti:sapphire sources.

IV. HHG IN A TWO-COLOR SCHEME

Exploiting the tunability of our near-ir parametric source, we were able to shift the central frequency of the driving pulses in a wide range between 1.4 and 1.6 μm without significantly affecting pulse energy and duration. Inset of Fig. 3(a) shows two spectra of the parametric source tuned around 1.5 μm (dashed curve) and 1.6 μm (solid curve), respectively. The measured pulse duration was $\sim$20 fs in both cases. The pulse peak intensity in the harmonic generation region was $\sim 2 \times 10^{14}$W/cm^2 for both central wavelengths. In Fig. 3 the harmonic spectra generated in krypton (a) and argon (b) by 1.5 μm (dashed curve) and 1.6 μm (solid curve) driving pulses are reported. The usual structure of odd harmonics is clearly visible. For both generating me-

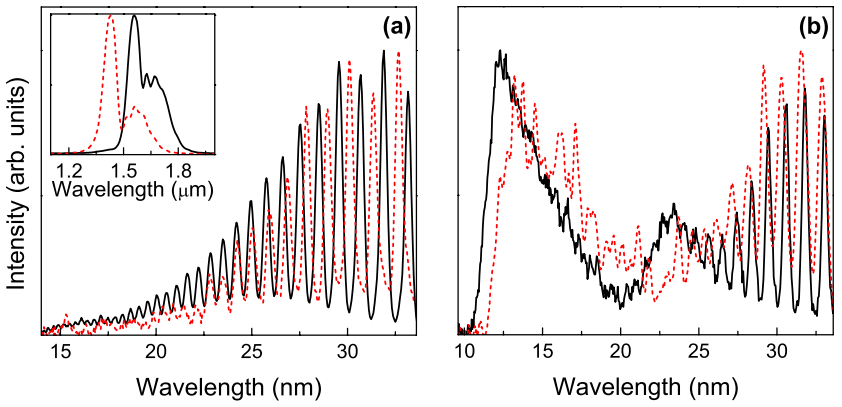

FIG. 3. (Color online) (a) High-order harmonic spectra generated in krypton by ir pulses with central wavelength tuned around 1.5 μm (dashed curve) and 1.6 μm (solid curve). Inset shows spectra of the two corresponding driving pulses with the same line styles. (b) High-order harmonic spectra generated in argon by ir pulses with central wavelength tuned around 1.5 μm (dashed curve) and 1.6 μm (solid curve).

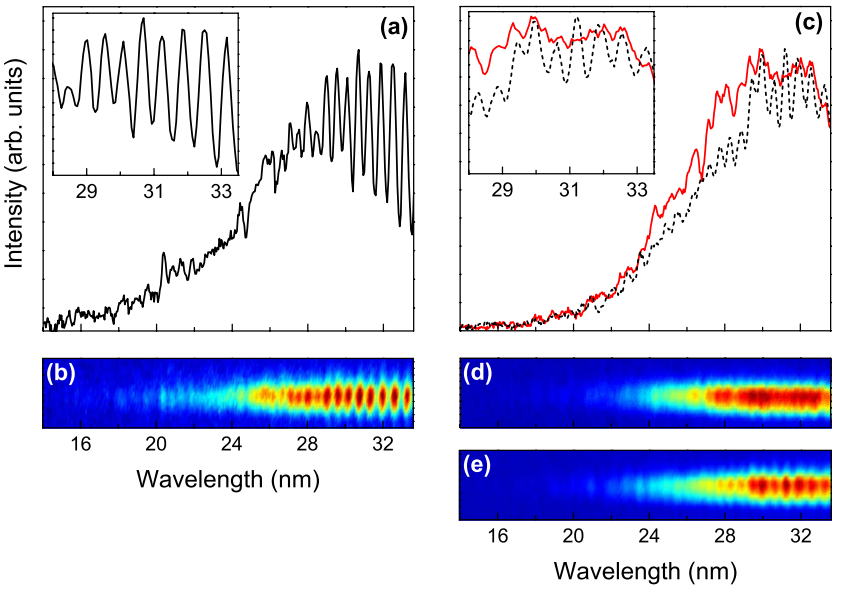

FIG. 4. (Color online) (a) Single-shot high-order harmonic spectrum generated in krypton by a 1.6 μm+800 nm driving pulse. Inset shows a detail of the spectrum. (b) Single-shot two-dimensional spectral image corresponding to measurement reported in (a). (c) Single-shot high-order harmonic spectra generated in krypton by a 1.5 μm+800 nm driving pulse for two different shots. A detail of the spectra is shown in the inset. [(d) and (e)] Single-shot two-dimensional spectral images corresponding to measurements reported in (c).

dia the longer wavelength driving pulse presents an extension of the cutoff frequency, as predicted by the cutoff law. It is worth pointing out that a tunability of the order of 100 nm around 1.5 μm in the driving wavelength corresponds to a complete tunability of the harmonic peaks in the spectral region above 25 eV.

The demonstrated carrier tunability was a fundamental prerequisite for HHG measurements in a two-color driving pulse configuration. The driving pulse was obtained by mixing the near-ir pulses generated by the parametric source with a small portion of the fundamental Ti:sapphire laser beam. The two components of the driving field were synchronized with a delay line; the polarization direction of the two beam was set parallel by means of a half-wave plate. Since Ti:sapphire pulses are not CEP stabilized, we expected a change in the overall driving field due to shot-to-shot CEP fluctuations of the 800 nm component; for this reason we acquired single-shot harmonic spectra. The 800 nm pulse had a peak intensity in the harmonic generation region lower than $\sim 3 \times 10^{13}$ W/cm^2; indeed this component was not able to produce by itself any detectable xuv emission. Adding the 800 nm component to the 1.6 μm driving pulse leads to field symmetry breaking, which corresponds to the appearance of even harmonics in the HHG process. This effect is evident in Fig. 4(a), which shows the xuv spectrum obtained in krypton. Panel (b) of the same figure shows the corresponding two-dimensional acquired spectral image, which evidences the discrete nature of the spectrum. The spectrum appears peakless for wavelengths shorter than 28 nm while the even and odd harmonic structures are clearly distinguishable for longer wavelengths [see inset of Fig. 4(a)]. In the case of a spectrum with even and odd harmonics of 1.6 μm we can estimate that our detection system was able to distinguish between different harmonic peaks corresponding to energies up to $\sim$50 eV. In this estimation we did not take into account the broadening of harmonic peaks with harmonic order, which could further reduce the spectral resolution in the short-wavelength region for multicycle driving pulses [36]. CEP fluctuations in the 800 nm component of the driving field did not affect significantly the harmonic spectral features: even and odd harmonics were always visible in all the single-shot measured spectra. This result is expected, since both the ir and the 800 nm components are not single-cycle pulses.

A completely different situation appeared when we tuned the near-ir source to 1.5 μm and we added the 800 nm component to the driving field. In this case the acquired spectra showed a clear even and odd harmonic structures for some shots and a broad continuum for some other shots. We attributed this behavior to CEP shot-to-shot fluctuations in the 800 nm component. Figure 4(c) shows two xuv spectra generated in krypton for two particular shots of the 1.5 μm+800 nm driving source. In the spectral region were the harmonic should be discernible, a broad continuum appears in one case

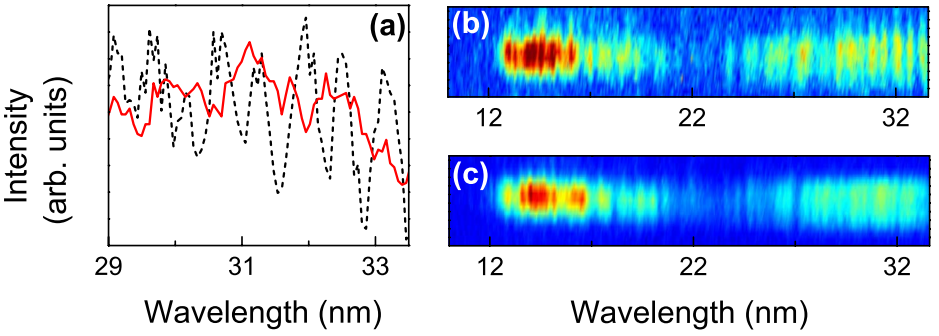

FIG. 5. (Color online) Left panel: portion of the single-shot high-order harmonic spectrum generated in argon by a 1.6 μm +800 nm driving pulse (black dashed curve) and by a 1.5 μm +800 nm driving pulse (red solid curve). Right panels: single-shot two-dimensional spectral images corresponding to measurements reported in (a).

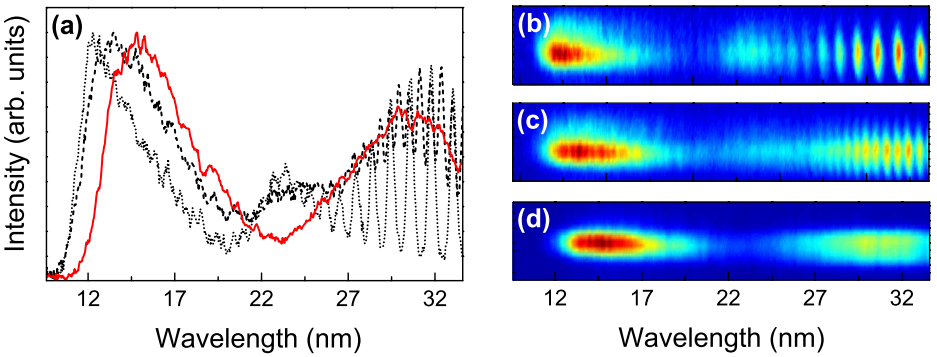

FIG. 6. (Color online) (a) High-order harmonic spectra generated in argon by 1600 nm pulses (black dotted curve), 1.6 μm +800 nm two-color pulses (black dashed curve), and 1.5 μm +800 nm two-color pulse (red solid curve). [(b), (c), and (d)] Two-dimensional spectral images corresponding, respectively, to 1600 nm, 1.6 μm+800 nm, and 1.5 μm+800 nm driving pulses.

(red solid curve) while in the other shot the spectrum appears to be modulated (black dashed curve) [see inset of Fig. 4(c)]. This is evidenced by the two-dimensional acquired spectral images shown in Figs. 4(d) and 4(e). It is worth noting that, though the spectrometer resolution was not enough in the high photon energy region, an xuv continuous spectrum at low photon energies is expected to be continuous in the whole energy range we observed (thus up to the cutoff wavelength of ~16 nm corresponding to ~70 eV). Indeed, the mechanism responsible for continuous xuv emission can be identified in the temporal gating produced by the two-color pulse [20]. In HHG by a multicycle driving pulse, harmonic emission occurs every half optical cycle due to the symmetry of the process. If the driving field consists of two components with different wavelengths, the periodicity of the process changes correspondingly to the change in the electric field shape. This could lead to emission of higher xuv photon energies only by a pulse slice around the peak of the driving field. Thus a continuous spectrum observed at lower xuv photon energies implies an xuv continuum also in the high photon energy region, where spectral resolution is lower.

Similar results were observed in single-shot harmonic measurements in argon, as reported in Fig. 5. We show in panel (a) the harmonic spectra generated by a 1.6 μm +800 nm driving field (black dashed curve) and by 1.5 μm+800 nm driving field (red solid curve) in the spectral region around 30 nm. The two-dimensional acquired images corresponding to the measurements reported in Fig. 5(a) are shown in Figs. 5(b) and 5(c), respectively. While in Fig. 5(b) the spectrum evidences the discrete harmonic peaks, in Fig. 5(c) the modulation corresponding to even and odd harmonics has vanished.

Owing to the lower harmonic yield in argon, the single-shot results are noisier as compared to the krypton ones. Nevertheless a comparison between spectra reported in Fig. 5(a) indicates that for some values of the 800 nm component CEP the harmonic spectrum becomes continuous. It is worth pointing out that in the case of argon we expect the harmonic spectrum to be continuous for xuv wavelengths shorter than 30 nm, up to the cutoff wavelength at 12 nm (~103 eV).

In order to better clarify the contribution of the CEP fluctuations of the 800 nm component in harmonic generation, we report in Fig. 6(a) the harmonic spectra generated in argon by 1.6 μm pulses (black dotted curve), 1.6 μm +800 nm (black dashed curve) and 1.5 μm+800 nm driving pulses (red solid curve). In these cases each spectrum is the result of integration over 40 laser shots. Corresponding two-dimensional acquired spectral images are reported in panels (b), (c), and (d), respectively. Even averaging the HHG emission over several laser shots, we were able to observe an evident harmonic modulation for 1.6 μm +800 nm driving pulses, whereas in the case of 1.5 μm +800 nm driving pulses the harmonic structure is completely smeared out.

V. CONCLUSIONS

In this work we reported on HHG performed by a high-energy self-phase-stabilized near-ir parametric source. The experimental results show a dramatic extension of the cutoff photon energy with respect to a standard Ti:sapphire laser source in atoms and small molecules. We performed single-shot two-color driven HHG experiment in argon and krypton by mixing the ir and 800 nm components available in our setup. We demonstrated the capability of controlling the harmonic emission process by changing the near-ir central frequency. Depending on the CEP of the two-color driving field components, we observed a discrete harmonic structure or a broad continuum extending from 16 to 34 nm in krypton. Broad continuous spectra (from 12 to 34 nm) were also reported in the case of argon. The combination of these results opens new and encouraging perspectives for the extension of attosecond physics toward the soft x-ray spectral region and for the investigation of quantum effects in atoms and molecules on a broader range of photon energies with respect to the state of the art. A very intriguing improvement of our approach for xuv continuum generation will be made possible exploiting the broad amplification bandwidth of our CEP-stabilized parametric source. By splitting the broadband seed of the source and amplifying two different spectral portions of the seed, it will be possible to produce a two-color driving pulse for HHG with passive CEP stabilization of both components. One could then control the driving electric field shape by changing the relative CEP of the two components thus finding the optimal condition for isolated attosecond pulse generation.

ACKNOWLEDGMENTS

We acknowledge the financial support from the Italian Ministry of Research (Project PRIN No. 2006027381) and the partial support from the European Union within Contract No. RII3-CT-2003-506350 (Laserlab Europe).

[1] E. Takahashi, Y. Nabekawa, and K. Midorikawa, Opt. Lett. **27**, 1920 (2002).
[2] E. A. Gibson, A. Paul, N. Wagner, R. Tobey, I. P. Christov, D. T. Attwood, E. Gullikson, A. Aquila, M. M. Murnane, and H. C. Kapteyn, Science **302**, 95 (2003).
[3] G. Sansone, E. Benedetti, F. Calegari, C. Vozzi, L. Avaldi, R. Flammini, L. Poletto, P. Villoresi, C. Altucci, R. Velotta, S. Stagira, S. De Silvestri, and M. Nisoli, Science **314**, 443 (2006).
[4] E. Goulielmakis, V. S. Yakovlev, A. L. Cavalieri, M. Uiberacker, V. Pervak, A. Apolonski, R. Kienberger, U. Kleineberg, and F. Krausz, Science **317**, 769 (2007).
[5] P. B. Corkum, Phys. Rev. Lett. **71**, 1994 (1993).
[6] M. Lewenstein, Ph. Balcou, M. Yu. Ivanov, A. L'Huillier, and P. B. Corkum, Phys. Rev. A **49**, 2117 (1994).
[7] B. Shan and Z. Chang, Phys. Rev. A **65**, 011804(R) (2001).
[8] E. Takahashi, T. Kanai, Y. Nabekawa, and K. Midorikawa, Appl. Phys. Lett. **93**, 041111 (2008).
[9] T. Popmintchev, M. Chen, O. Cohen, M. E. Grisham, J. J. Rocca, M. M. Murnane, and H. C. Kapteyn, Opt. Lett. **33**, 2128 (2008).
[10] H. Xu, H. Xiong, Z. Zeng, Y. Fu, J. Yao, R. Li, Y. Cheng, and Z. Xu, Phys. Rev. A **78**, 033841 (2008).
[11] V. Tosa, private communication.
[12] J. Tate, T. Auguste, H. G. Muller, P. Saliéres, P. Agostini, and L. F. DiMauro, Phys. Rev. Lett. **98**, 013901 (2007).
[13] K. Schiessl, K. L. Ishikawa, E. Persson, and J. Burgdorfer, Phys. Rev. Lett. **99**, 253903 (2007).
[14] P. Colosimo, G. Doumy, C. I. Blaga, J. Wheeler, C. Hauri, F. Catoire, J. Tate, R. Chirla, A. M. March, G. G. Paulus, H. G. Muller, P. Agostini, and L. F. DiMauro, Nat. Phys. **4**, 386 (2008).
[15] V. S. Yakovlev, M. Ivanov, and F. Krausz, Opt. Express **15**, 15351 (2007).
[16] R. Kienberger, E. Goulielmakis, M. Uiberacker, A. Baltuska, V. Yakovlev, F. Bammer, A. Scrinzi, Th. Westerwalbesloh, U. Kleineberg, U. Heinzmann, M. Drescher, and F. Krausz, Nature (London) **427**, 817 (2004).
[17] I. J. Sola, E. Mével, L. Elouga, E. Constant, V. Strelkov, L. Poletto, P. Villoresi, E. Benedetti, J.-P. Caumes, S. Stagira, C. Vozzi, G. Sansone, and M. Nisoli, Nat. Phys. **2**, 319 (2006).
[18] N. Dudovich, O. Smirnova, J. Levesque, Y. Mairesse, M. Y. Ivanov, D. M. Villeneuve, and P. B. Corkum, Nat. Phys. **2**, 781 (2006).
[19] Z. Zeng, Y. Cheng, X. Song, R. Li, and Z. Xu, Phys. Rev. Lett. **98**, 203901 (2007).
[20] H. Merdji, T. Auguste, W. Boutu, J.-P. Caumes, B. Carré, T. Pfeifer, A. Jullien, D. Neumark, and S. Leone, Opt. Lett. **32**, 3134 (2007).
[21] B. Kim, J. Ahn, Y. Yu, Y. Cheng, Z. Xu, and D. E. Kim, Opt. Express **16**, 10331 (2008).
[22] A. Baltuška, T. Fuji, and T. Kobayashi, Phys. Rev. Lett. **88**, 133901 (2002).
[23] C. Manzoni, C. Vozzi, E. Benedetti, G. Sansone, S. Stagira, O. Svelto, S. De Silvestri, M. Nisoli, and G. Cerullo, Opt. Lett. **31**, 963 (2006).
[24] T. Fuji, N. Ishii, C. Y. Teisset, X. Gu, T. Metzger, A. Baltuška, N. Forget, D. Kaplan, A. Galvanauskas, and F. Krausz, Opt. Lett. **31**, 1103 (2006).
[25] C. Vozzi, G. Cirmi, C. Manzoni, E. Benedetti, F. Calegari, G. Sansone, S. Stagira, O. Svelto, S. De Silvestri, M. Nisoli, and G. Cerullo, Opt. Express **14**, 10109 (2006).
[26] C. P. Hauri, R. B. Lopez-Martens, C. I. Blaga, K. D. Schultz, J. Cryan, R. Chirla, P. Colosimo, G. Doumy, A. M. March, C. Roedig, E. Sistrunk, J. Tate, J. Wheeler, L. F. DiMauro, and E. P. Power, Opt. Lett. **32**, 868 (2007).
[27] C. Vozzi, F. Calegari, E. Benedetti, S. Gasilov, G. Sansone, G. Cerullo, M. Nisoli, S. De Silvestri, and S. Stagira, Opt. Lett. **32**, 2957 (2007).
[28] C. Vozzi, C. Manzoni, F. Calegari, E. Benedetti, G. Sansone, G. Cerullo, M. Nisoli, S. De Silvestri, and S. Stagira, J. Opt. Soc. Am. B **25**, B112 (2008).
[29] C. Altucci, R. Bruzzese, C. de Lisio, M. Nisoli, E. Priori, S. Stagira, M. Pascolini, L. Poletto, P. Villoresi, V. Tosa, and K. Midorikawa, Phys. Rev. A **68**, 033806 (2003).
[30] J. Itatani, J. Levesque, D. Zeidler, H. Niikura, H. Pépin, J. C. Kieffer, P. B. Corkum, and D. M. Villeneuve, Nature (London) **432**, 867 (2004).
[31] T. Kanai, S. Minemoto, and H. Sakai, Nature (London) **435**, 470 (2005).
[32] C. Vozzi, F. Calegari, E. Benedetti, J. P. Caumes, G. Sansone, S. Stagira, M. Nisoli, R. Torres, E. Heesel, N. Kajumba, J. P. Marangos, C. Altucci, and R. Velotta, Phys. Rev. Lett. **95**, 153902 (2005).
[33] R. Torres, N. Kajumba, J. G. Underwood, J. S. Robinson, S. Baker, J. W. G. Tisch, R. de Nalda, W. A. Bryan, R. Velotta, C. Altucci, I. C. E. Turcu, and J. P. Marangos, Phys. Rev. Lett. **98**, 203007 (2007).
[34] X. Zhou, R. Lock, W. Li, N. Wagner, M. M. Murnane, and H. C. Kapteyn, Phys. Rev. Lett. **100**, 073902 (2008).
[35] W. Boutu, S. Haessler, H. Merdji, P. Breger, G. Waters, M. Stankiewicz, L. J. Frasinski, R. Taieb, J. Caillat, A. Maquet, P. Monchicourt, B. Carre, and P. Salieres, Nat. Phys. **4**, 545 (2008).
[36] E. Priori, G. Cerullo, M. Nisoli, S. Stagira, S. De Silvestri, P. Villoresi, L. Poletto, P. Ceccherini, C. Altucci, R. Bruzzese, and C. de Lisio, Phys. Rev. A **61**, 063801 (2000).